Journal of Ultrafine Grained and Nanostructured Materials
https://jufgnsm.ut.ac.ir
Vol. 56, No.1, June 2023, pp. 99-107
Print ISSN: 2423-6845 Online ISSN: 2423-6837
DOI: 10.22059/jufgnsm.2023.01.10

The effect of TiO_2 nanotubes on the biological properties of porous titanium foam by anodization technique for orthopedic application

Roghayeh Haghjoo[1], Seyed Khatiboleslam Sadrnezhaad [2*], Nahid Hassanzadeh Nemati[1]

[1]Department of Biomedical Engineering, College of Medical Science and Technologies, Science and Research Branch, Islamic Azad University, Tehran, Iran
2Department of Materials Sciences, Sharif University of Technology, Tehran, Iran

Recieved: 9 September 2022; Accepted: 25 January 2023

**Corresponding author email: sadrnezh@sharif.edu*

ABSTRACT

In the present study, the TiO_2 nanotubes were grown on the surface of porous titanium foam by the anodization method. The surface of titanium foam before and after the coating of TiO_2 nanotubes was structurally and morphologically characterized by X-ray diffraction (XRD), field emission electron microscope (FESEM) equipped with energy-dispersive X-ray (EDX). Additionally, the cytocompatibility of TiO_2-coated porous titanium foam was evaluated by methyl thiazol tetrazolium (MTT) assay. The results have shown that the anatase crystalline phase was formed on the surface with a uniform thickness of 2.5 µm. Finally, TiO_2-coated porous titanium foam was biocompatible and significantly enhanced the proliferation and attachment of MG-63 osteoblast cells compared to the uncoated substrate. All the results postulated that the coating of titanium substrate with TiO_2 nanotube shows excellent promise for orthopedic implant application.

Keywords: *Titanium foam, Bone implant, Powder metallurgy, Nanotube, Cytocompatibility*

1.Introduction

According to the powder metallurgy, to acquire a porous structure, the technique with space holder is used as a considerable method[1]. Space holder particles are employed as the pore former in porous metal foams. Thus, the space holder method is utilized in controlling the parameters related to porosity comprising its morphology and the percentage of pore dispersion. For this purpose, a wide range of space holders like saccharose, urea [2], and starch have been used. The space holder can be easily removed and rapidly dissociated with little residual, making it more advantageous over other pore-making techniques.

Titanium implants have been widely used as dental bone implants [3]. Nonetheless, its higher density and rigidity compared to natural human bone leads to implant loosening and, consequently implant fracture [4]. Porous titanium possesses unique characteristics, including a large specific surface area, low density, and a high strength-to-weight ratio [5]. In addition, the porous structure can be alternatively used to repair bone defects due to their biocompatibility and comparable stiffness to that of human bone [6]. In this regard, porous titanium can enhance implant fixation

and accelerate bone healing which caused by the substitution of the bone tissue ingrowth to the pores [7].

Surface treatment is required to improve the surface properties of metallic implant [8]. One way to enhance the surface quality is to add materials with favorable properties, such as nanostructured material. For this purpose, by adding nanostructured materials to the implant surface, the cell fate can be controlled and the osteoconductivity of the implant can be promoted by increasing the interactions with serum proteins [9]. One of the potential nanostructured materials is titanium dioxide (TiO_2). There are some notable properties of TiO_2-based materials such as nontoxicity, biocompatibility, large surface area, and chemical stability [10]. However, the main disadvantage of TiO_2 nanoparticles is poor recyclability and secondary pollution due to their difficult separation [11]. The immobilization of TiO_2 on the solid surface, including metals has been proposed to tackle this challenge [11]. Although the expensive phase separation process is eliminated by using this approach, the specific surface area of TiO_2 is significantly reduced. Consequently, researchers have attempted to fabricating porous TiO_2 on the substrate to enhance the specific surface area [12].

Various techniques can be employed to immobilize the nanostructured material on the surface of titanium implants, such as micro-arc oxidation, plasma spraying, magnetron sputtering, and anodization [13]. The anodizing technique is also used to increase the thickness and regularity of the oxide layer on the implant's surface [12]. An extensive body of literature in recent years showed that the fabrication of TiO_2 nanotube by anodization significantly improved the osteoblastic activity of the porous titanium scaffold [14, 15]. However, in most of the reports, anodic oxidation was mainly used to deal with dense titanium and titanium alloy, not porous titanium. Nonetheless, Fan X et al. [16] investigated the bioactivity of the TiO_2 nanotubes on the porous titanium by in vitro and in vivo evaluations.

In our previous study, TiO_2 nanoparticles was coated on the surface of titanium foam using magnetron sputtering, and the results illustrated an improvement in the biological properties of titanium foam [17]. Therefore, this study aimed to fabricate porous titanium foam using powder metallurgy and urea as the space holder and explore the effect of TiO_2 nanotube formation by anodic oxidation on the foam surface in improving the chemical, physical, and biological properties of the samples. It is expected that this macro-pores and nanotubes can significantly improve the bioactivity of porous titanium. The bioactivity of the TiO_2 nanotubes on the porous titanium was investigated by in vitro evaluation.

2. Materials and methods

Titanium hydride (TiH_2) powder with an average particle size of 45 μm and urea powder with Needle-like morphology as a space holder (with size of the particle from 500 up to 800 micrometers) were used as raw materials. Ethylene glycol ($C_2H_6O_2$), Ammonium fluoride (NH_4F), Sodium carbonate (Na_2CO_3) were electrolyte for anodic oxidation. Also, double distilled water (ddH_2O) was applied in all the aqueous solutions. Table 1 summarizes the information on these materials.

2.1. Preparation of foams

The foam with needle-shape, morphology was

Table 1- Types of materials employed in the present study

Materials	Use to make	Ordered company
(TiH_2) powder	titanium foam	Merck (Darmstadt, Germany)
urea powder (CH_4N_2O)	titanium foam	Sinchem South Korea
Ethylene glycol ($C_2H_6O_2$)	electrolyte for anodic oxidation	Merck (Darmstadt, Germany)
Ammonium fluoride (NH_4F)	electrolyte for anodic oxidation	Merck (Darmstadt, Germany)

fabricated using titanium hydride (TiH_2) and needle-shaped urea space holder. For this purpose, the space holder was mixed with TiH_2 with a volume ratio of 5:5. Then, green pellets were prepared by uniaxial compression of the powder mixture under pressure of 120 MPa to produce a green specimen with a height of 5 mm and a diameter of 8 mm, which is based on the standard compression test of metallic materials at room temperature (E9-89a, ASTM). Specimens with the same dimensions were prepared for biological tests. Afterward, a sintering process was applied to remove the remaining space holder material and sinter the particles of the green specimen. The temperature was increased at the rate of 278.15 $kmin^{-1}$ from the room temperature to 200 °C and was maintained for 40 min to evaporate the urea space holder. Under 10^{-4} torr vacuum pressure, the temperature was elevated to 1000 °C and was maintained for 3 h to sinter the sample.

2.2. Anodizing process

All the anodization experiments were carried out at room temperature in a two-electrode electrochemical cell. The initial specimens were cylindrical titanium foam with a height of 5 mm and a diameter of 8 mm as anode and graphite thin film with thickness of 1 mm as cathode. Before anodizing, titanium foam was sanded with abrasive papers from 600 to 2000 and polished with solution containing Al_2O_3 particles (0.3 mm). Then, it was rinsed with acetone and ethanol (volume ratio 1:1), afterwards, it was washed with deionized water and finally dried at ambient temperature. All the experiments were performed at the constant DC voltage of 60 V for 1.5 h. Area ratio of anode to cathode was 1:1 and distance between them was fixed as 3 cm. The used electrolyte includes ethylene glycol, 3 vol% of deionized water, NH_4F (0.3 M) and sodium carbonate (0.03 M).

2.3.1. Structural analysis

The phase analysis of pure porous titanium foams and TiO_2-coated titanium foams were performed by X-ray diffraction (XRD, EQUINOX 3000, France), and the XRD patterns were obtained by Cu-Kα radiation with diffraction angles $20° \leq 2\theta \leq 80°$. Then, the patterns were matched to the International Centre for Diffraction Data (ICDD) reference file using PANalytical X'Pert Highscore Plus software. An energy-dispersive X-ray (EDX) (FESEM, TESCAN-XMU, Czech Republic) device was employed to assess chemical composition.

2.3.2. Morphological properties

The microstructure and morphology of porous titanium foams were evaluated by light microscope (Olympus CX23 Japan microscope) and the morphology and structure of the TiO_2 arrays were investigated by field emission electron microscope (FESEM, TESCAN-XMU, Czech Republic). Before FESEM observation, Au was sputtered on the surface of the specimens.

2.3.3. Physical properties

The fabricated foam's relative density and apparent porosity were calculated using Archimedes principles according to ASTM B962-17 [18]. The specimens were weighed accurately, immersed in distilled water, and reweighed. The porosity was determined by calculating the weight difference of samples before and after water immersion. Equations 1 to 5 were used to calculate volumetric density (D_b), solid bulk density (D_{sb}), open porosity (P_a), total porosity (P_t), total porosity (P_c), respectively. Where D_1 was water density, D_t was theoretical density, W_e was wet weight, W_a was sample dry weight, W_b was immersion weight, the theoretical density of solid titanium was reported to be 4.506 g/cm^3 and the theoretical density of porous titanium foam was reported to be 4.506 g/cm^3 [19].

$$D_b = (W_a / W_e - W_b) \times D_1 \quad \text{(eq. 1)}$$

$$D_{as} = (W_a / W_a - W_b) \times D_1 \quad \text{(eq. 2)}$$

$$P_a = 100 \times (1 - D_b / D_{as}) \quad \text{(eq. 3)}$$

$$P_t = 100 \times (1 - D_b / D_t) \quad \text{(eq. 4)}$$

$$P_c = P_t - P_a \quad \text{(eq. 5)}$$

2.3.4. In vitro cell biocompatibility assay

The in vitro biocompatibility assay was conducted based on International Organization for Standardization (ISO) 10993: Biological Evaluation of Medical Devices, Part 5: Tests for Cytotoxicity [20]. For this purpose, the experiments were carried out in 96-well culture plates. The MG-63 (NCBI C-116, National Cell Bank of Iran, Pasteur Institute, Iran) was cultured at 3×10^4 cells/sample density. The medium used for culturing these cells was a mix of Dulbecco's Modified Eagle Medium (DMEM, GIBCO, and Scotland) and Ham's F-12 supplemented with 10% fetal bovine serum (Seromed, Germany), 100 µg/mL streptomycin, and 100 U/penicillin (Sigma, USA). The cultures were incubated for different time durations. At the end of culture time, the

cells were harvested for 3-(4,5-dimethylthiazol-2-yl)-2, 5-diphenyltetrazolium-bromide (MTT) proliferation assay and field emission scanning electron microscope (FESEM).

2.3.4.1. MTT assay for cell viability and proliferation

The control sample was a tissue culture polystyrene plate (TCPS), and the assay was MTT. Each cylindrical sample with a height of 5 mm and a diameter of 8 mm was seeded at a cell density of 5×10^3 by using a 24-well plate. After 3 and 7 days, the culture medium was removed from each well, and 1 mL of MTT solution (0.5 $mgmL^{-1}$, Sigma, USA) was added. Next, the medium was placed in the incubator at 37° C for 5 h. The wells were placed on a shaking incubator for 15 min to reach optimal absorbance measurement. In addition, to dissolve the purple formazan crystals, 1 mL isopropanol (Sigma, USA) was added to each well. At this point, the optical density was recorded at 545 nm using a multi-well microplate reader (STAT FAX 2100, USA). This procedure was repeated three times, and the final ODs were normalized to control the optical density.

2.3.4.2. Cell morphology

The cells were cultured for 24 h, fixed in 2.5 % glutaraldehyde, and dehydrated for 10 min using alcohols graded 50 %, 70 %, 80 %, 85 %, 90 %, 95 %, and 100 %. First, samples were examined by optical light microscopy. Second, the specimens were sputter-coated with gold and were examined using a FESEM.

2.3.5. Statistical analysis

The data were statistically analysed by the analysis of variance (ANOVA) using the SPSS software version 22. P-value <0.05 was considered significant for all tests.

3. Results and discussion

Figure 1 shows the light microscope images of needle-like urea and the corresponding titanium porous foam fabricated by powder metallurgy and needle-like urea as the space holder. The size of macropores was found to be in the range of 400-700 μm. This pore size is suitable for attachment, proliferation, and growth of osteoblast [21]. The formation of open and interconnected pores is the decomposition of urea into the water, carbon dioxide, and NH_3 under heat treatment. Table 1 shows the porosity parameters of both titanium foams and titanium samples without macropores. Despite the lower porosity of the titanium sample (26 % according to Table 1), titanium foams had an open pore network of 60.2 %. It has been reported [22] that pores in porous metals could be divided into two types: the micro-pores and the macro-pores. The former is generated due to the partial sintering of TiH_2 powders and have resulted from TiH_2 decomposition. These results supported the findings of Akbarinia et al. and Naddaf et al. [23, 24] that presented the decomposition of hydride molecules helps form highly active newly created titanium sites at the exterior of the hydride particles. On the other hand, the latter that has much larger

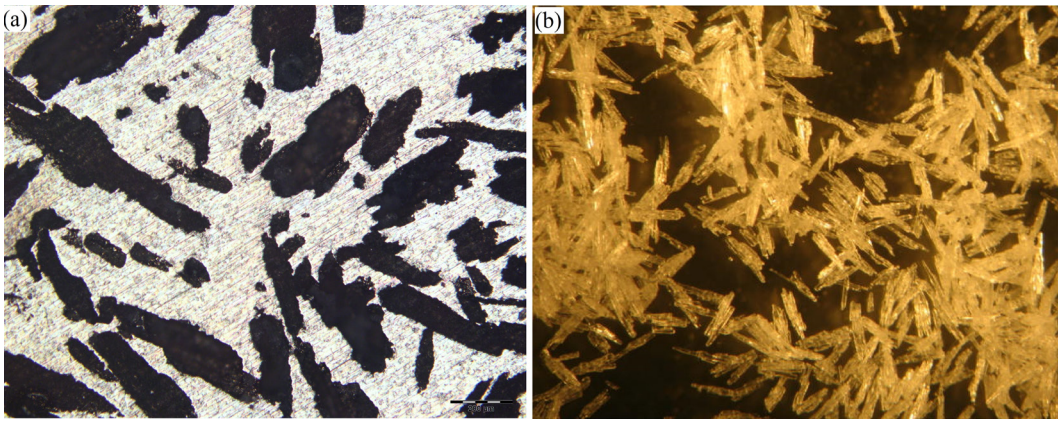

Fig. 1- Light microscope images of (a) titanium foam and (b) needle-like urea powder.

Table 2- Porosity parameters of titanium foams and titanium samples without macropores

Samples	Total porosity (%)	Open pores (%)	Closed pores (%)	Density (gcm^3)
Ti	26.25	15.16	10.09	2.84
Ti/NU	60.2	31	29.2	1.793

size are obtained by the decomposition of spacer particles. Therefore, the substrate's microporosity and macroporosity justify the implant's physicochemical and biological properties [25].

Figure 2 shows the XRD pattern of titanium foam and the titanium foam coated with titanium dioxide (TiO_2) using the anodizing method. The corresponding peaks related to the titanium substrate and titanium oxide layer with anatase crystalline phase can be observed. The structure of surface oxide obtained from the anodizing method is usually amorphous due to the rapid reactions during anodizing [26]. TiO_2 possesses three distinct phases including anatase, rutile, and brookite. It was found that the anatase phase initiates to form at around 300 °C, and its formation is completed at 600°C [27]. Further, an increase in the temperature leads to the formation of the rutile phase. The present study's peak at 2θ=25.1° with plane index (101) indicated the phase transformation to anatase crystalline phase in the surface oxide nanotubes after heat treatment at 480°C. According to previous reports, the anatase phase is more beneficial for bone growth than rutile due to network similarity to hydroxyapatite [27].

The FESEM micrographs of the cross-section

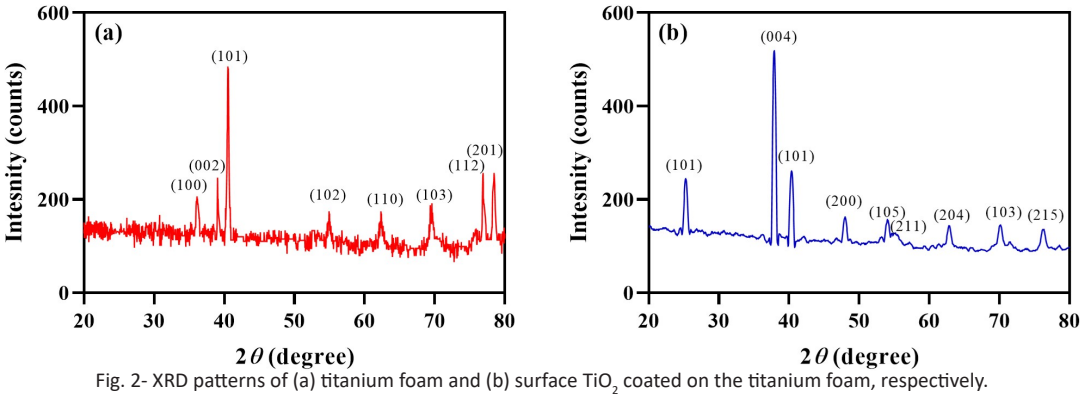

Fig. 2- XRD patterns of (a) titanium foam and (b) surface TiO_2 coated on the titanium foam, respectively.

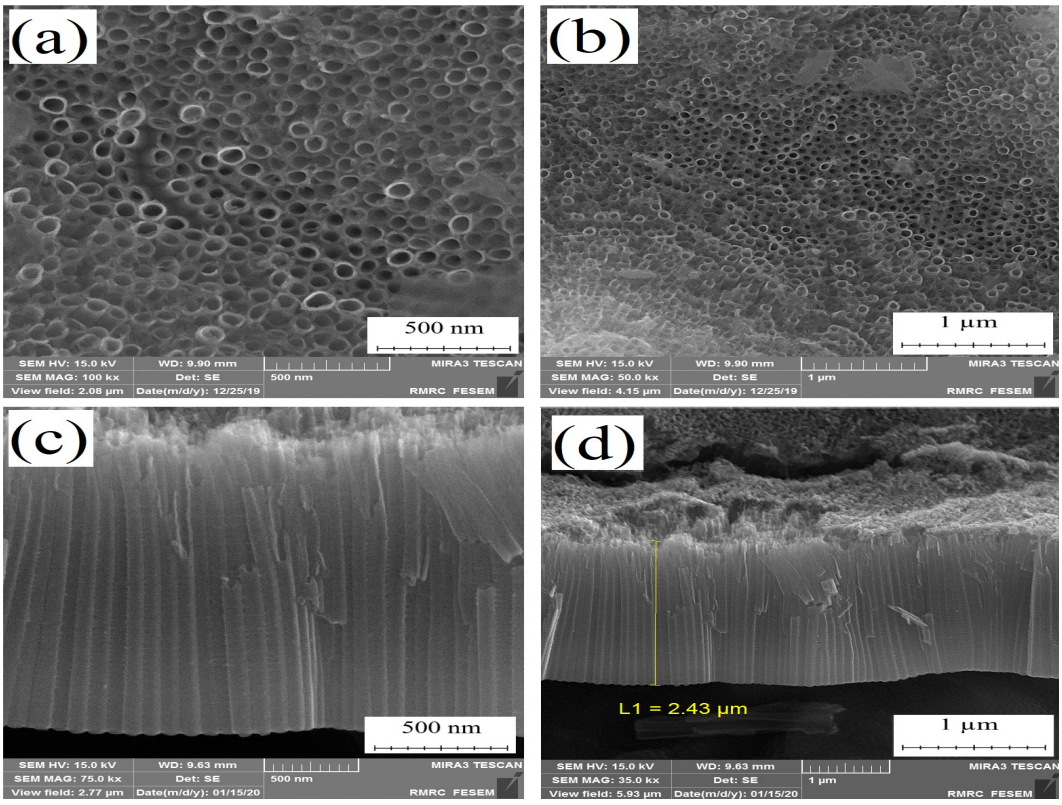

Fig. 3- FESEM micrograph of (a, b) top and (c,d) cross sections TiO_2 coated- titanium foam after anodizing process in different magnifications.

of titanium foam coated with TiO_2 layer using anodizing method are shown in Figure 3. As can be observed from the two different magnifications, the thickness of organized nanotubes with uniform walls was found to be 2.5 μm. These organized nanotubes were obtained by using an organic electrolyte in which sodium carbonate was added as the buffer not only to increase the thickness of nanotubes but also to reduce the internal diameter and ultimately improve the morphology of nanotubes [28]. However, according to the following reaction, the sodium ions could be present in the nanotubes as the impurities [29]:

$$Na_2CO_3 + 12F^- + 2H^+ \rightarrow 2[NaF_6]^{5-} + CO_2 + H_2O$$

NH_4F was used as the organic electrolyte to prevent the presence of such impurities. The EDX analysis of the titanium foam and nanostructured TiO_2 on the surface of titanium foam after the anodizing process is shown in Figure 4. As can be observed, there were no additional or unwanted elements in titanium foam before and after coating. Additionally, the presence of Ti and O elements with 55.94% and 44.06% weight percent, respectively indicated the formation of the TiO_2 layer on the titanium foam after anodizing process. According to EDX analysis, the powders were not oxide during sintering, which may lead to better mechanical properties for porous titanium foams.

Figure 5 shows the percentages of viable cells in different samples. The cell viability of control samples was considered 100 %. According to a previous report, the cell viability above 70%

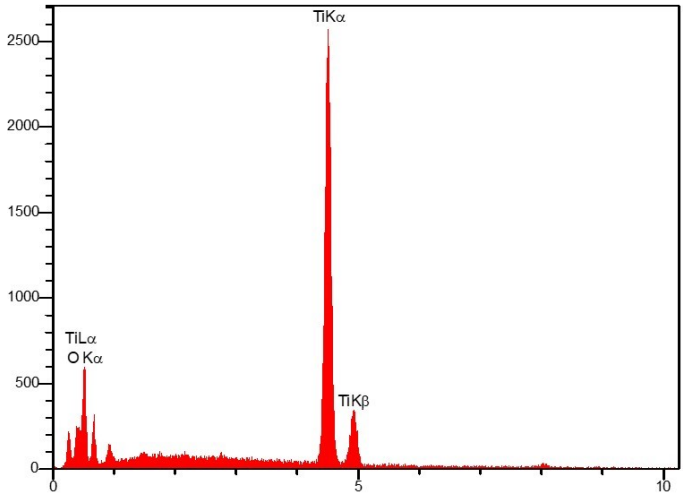

Fig. 4- The EDX analysis of nanostructured TiO_2 on the titanium foam using anodizing process.

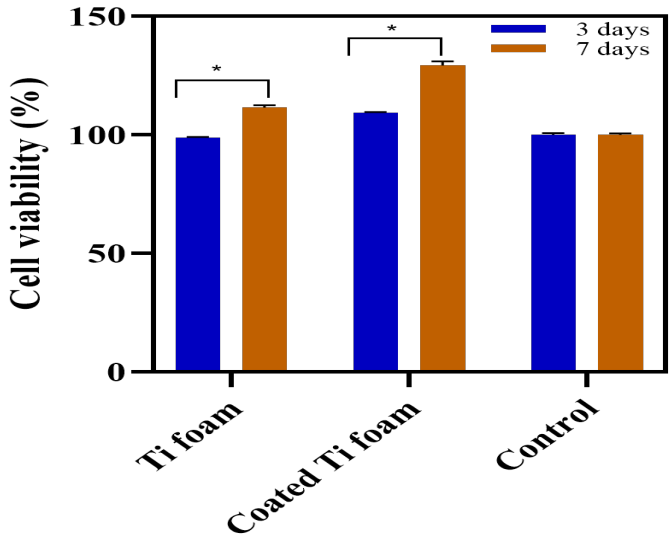

Fig. 5- MTT assay of human osteoblast (MG63) cells on the coated titanium and titanium foam without coating after 3 and 7 days of cell culture, respectively where * indicate the significant difference ($p^*<0.05$).

indicates the cytocompatibility of the sample [30]. The cell biocompatibility of osteoblast (MG63) cells on the titanium foam without spacer (control) and titanium foams prepared by needle-like urea spacers with nanotubes was evaluated by MTT assay, and the results are depicted in Figure 5. As can be seen, the titanium foam coated with nanotubes showed significantly higher cell viability compared to titanium foam without coating ($p^*<0.05$). Additionally, both revealed significantly higher cell viability than control samples. This high percentage of cell viability could be attributed to sufficient porosities as previous studies have demonstrated that the macropores of the implants are sufficiently enough for cell infiltration, nutrients, and metabolites [14]. In addition, the needle-like pore morphologies possessed sharp corners, which increased the implant's surface roughness and surface area. This leads to better adsorption of proteins and other biological molecules, which ultimately increases cell viability [21]. Van Bael et al. have reported that cells have bridging behavior which defines that the surface tension is inclined to reduce the curvature on the angled corner of the pores as much as possible to give the pores circular shapes [31]. To this end, the enhanced cell viability could be attributed to the bridging behavior of cells by which the cells are inclined to bridge on the angled corner of the pores. Although the titanium foams with needle pore morphology showed high cell viability compared to control samples, it is unclear in which pore morphology could provide better cellular behavior because different pore morphologies have been shown to adjust the properties of titanium -based orthopedic implants [32].

The coating of TiO_2 nanotubes using anodizing also enhanced the cell viability, indicating a nanotube, positive effect cell activity. The possible explanation for this enhancement in cell viability is the microstructural properties and the shape of the coating layer. The anodized layer with a nanometric structure provides a large specific surface area for cell activity and suitable porosity for MG63 cell anchorage and adhesion. It was found in previous studies that the pore surface and shape can affect osteoblast cell connectivity [28]. Additionally, the elevation in surface charge density on the sharp edges of TiO_2 nanotubes could improve the adhesion of mediating proteins as the positively-charged proteins on the corners could connect with the negatively-charged surface during electrostatic forces [33]. Therefore, we can draw a conclusion that nanotubes of anatase phase have positive effect

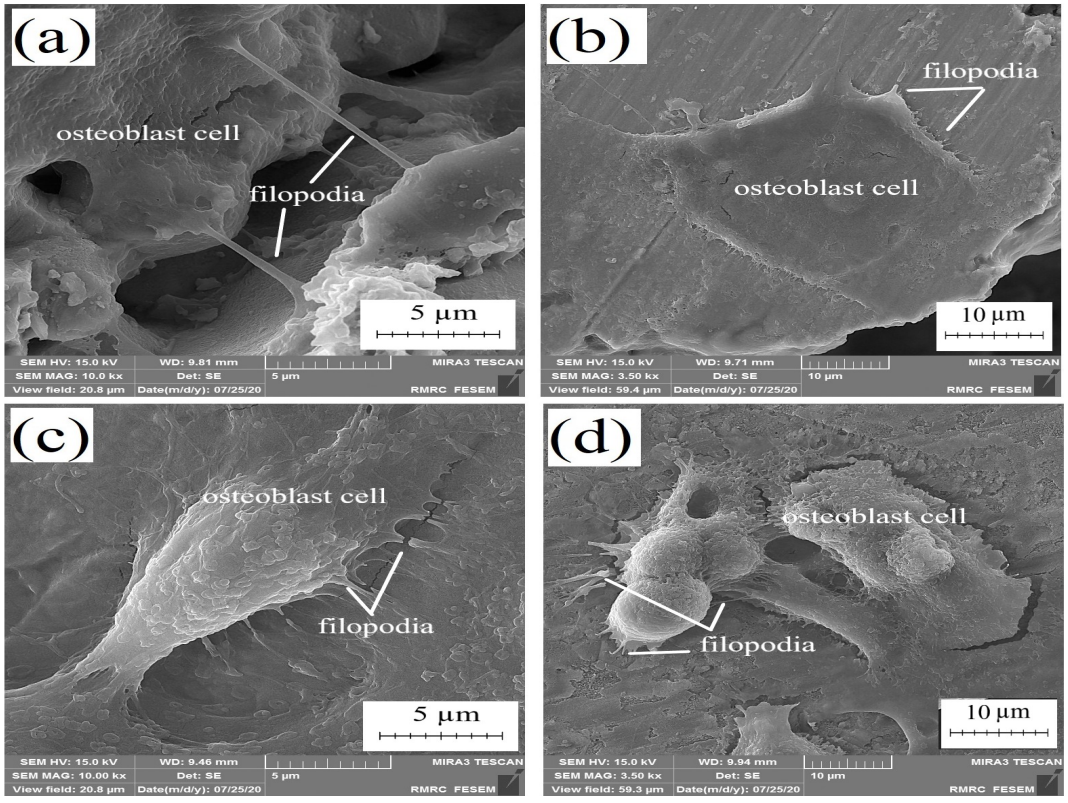

Fig. 6- FESEM micrographs of MG63 cell attachment on (a,b) titanium foam with needle-like pore morphology and (c,d) titanium foam coated with TiO_2 nanotubes at two different magnifications, respectively.

on the the enhanced cell viability of the implants and scaffolds because of their inducing ability to formation.

To further investigate the cellular response and their connectivity, the cells were observed by FESEM after 24 h. As shown in Figure 6, MG63 cells were all well attached on the surface titanium foams with and without TiO_2 nanotubes. The MG63 cells showed elongated filopodia on the surface, which is in good agreement with the MTT assay. In addition, the cells covered the surface. This indicated that the surface supported the cell attachment as the cells were elongated on the surface instead of maintaining their original shape (circular) [34].

4. Conclusion

In this study, titanium porous foam was fabricated by powder metallurgy using a needle-like urea space holder, and a thin layer of TiO_2 nanotube was successfully coated on the surface of porous titanium foam. The phase analysis indicated that the anatase crystalline phase was formed in the surface oxide nanotube. This occurrence was further confirmed by the presence of Ti and O elements in the coating indicating the formation of a TiO_2 layer on the titanium foam after the anodizing process. Finally, the coating of TiO_2 nanotubes using anodizing also significantly enhanced the cell viability and supported the proliferation and attachment of MG-63 osteoblast cells. The nanostructured TiO_2-coated metallic substrate showed excellent promise for bone and dental implant applications.

Acknowledgment

The authors acknowledge the Islamic Azad University Science and Research Branch for general support to obtain the experimental work.

References

1. Rodriguez-Contreras A, Punset M, Calero JA, Gil FJ, Ruperez E, Manero JM. Powder metallurgy with space holder for porous titanium implants: A review. Journal of Materials Science & Technology. 2021;76:129-49.

2. Qiu G, Wang J, Cui H, Lu T. Mechanical behaviors and porosity of porous Ti prepared with large-size acicular urea as spacer. SN Applied Sciences. 2018;1(1):107.

3. Lascano S, Arévalo C, Montealegre-Melendez I, Muñoz S, Rodriguez-Ortiz JA, Trueba P, et al. Porous Titanium for Biomedical Applications: Evaluation of the Conventional Powder Metallurgy Frontier and Space-Holder Technique. Applied Sciences. 2019;9(5):982.

4. Rivard J, Brailovski V, Dubinskiy S, Prokoshkin S. Fabrication, morphology and mechanical properties of Ti and metastable Ti-based alloy foams for biomedical applications. Materials Science and Engineering: C. 2014;45:421-33.

5. Ahmadi S, Sadrnezhaad S. A novel method for production of foamy core@ compact shell Ti6Al4V bone-like composite. Journal of Alloys and Compounds. 2016;656:416-22.

6. Perez RA, Mestres G. Role of pore size and morphology in musculo-skeletal tissue regeneration. Materials Science and Engineering: C. 2016;61:922-39.

7. Cetinel O, Esen Z, Yildirim B. Fabrication, morphology analysis, and mechanical properties of Ti foams manufactured using the space holder method for bone substitute materials. Metals. 2019;9(3):340.

8. Chappuis V, Maestre L, Bürki A, Barré S, Buser D, Zysset P, et al. Osseointegration of ultrafine-grained titanium with a hydrophilic nano-patterned surface: an in vivo examination in miniature pigs. Biomaterials science. 2018;6(9):2448-59.

9. Ahmadi S, Mohammadi I, Sadrnezhaad S. Hydroxyapatite based and anodic Titania nanotube biocomposite coatings: Fabrication, characterization and electrochemical behavior. Surface and Coatings Technology. 2016;287:67-75.

10. Minagar S, Berndt CC, Wang J, Ivanova E, Wen C. A review of the application of anodization for the fabrication of nanotubes on metal implant surfaces. Acta biomaterialia. 2012;8(8):2875-88.

11. Shan AY, Ghazi TIM, Rashid SA. Immobilisation of titanium dioxide onto supporting materials in heterogeneous photocatalysis: A review. Applied Catalysis A: General. 2010;389(1-2):1-8.

12. Shayegan Z, Lee C-S, Haghighat F. TiO2 photocatalyst for removal of volatile organic compounds in gas phase–A review. Chemical Engineering Journal. 2018;334:2408-39.

13. Chernozem RV, Surmeneva MA, Ignatov VP, Peltek OO, Goncharenko AA, Muslimov AR, et al. Comprehensive Characterization of Titania Nanotubes Fabricated on Ti–Nb Alloys: Surface Topography, Structure, Physicomechanical Behavior, and a Cell Culture Assay. ACS Biomaterials Science & Engineering. 2020;6(3):1487-99.

14. Mohan L, Dennis C, Padmapriya N, Anandan C, Rajendran N. Effect of Electrolyte Temperature and Anodization Time on Formation of TiO2 Nanotubes for Biomedical Applications. Materials Today Communications. 2020;23:101103.

15. Ahmadi S, Riahi Z, Eslami A, Sadrnezhaad SK. Fabrication mechanism of nanostructured HA/TNTs biomedical coatings: an improvement in nanomechanical and in vitro biological responses. J Mater Sci Mater Med. 2016;27(10):150.

16. Fan X, Feng B, Liu Z, Tan J, Zhi W, Lu X, et al. Fabrication of TiO2 nanotubes on porous titanium scaffold and biocompatibility evaluation in vitro and in vivo. Journal of Biomedical Materials Research Part A. 2012;100A(12):3422-7.

17. Haghjoo R, Sadrnezhaad SK, Nemati NH. Thin TiO2 Nanocoating of Porous Titanium through Radio Frequency Magnetron Sputtering to Improve the Biological Response of Orthopedic Implants. Journal of Clinical Research in Paramedical Sciences. 2021;10(2).

18. Committee B. ASTM B962-17 Standard Test Methods for Density of Compacted or Sintered Powder Metallurgy (PM) Products Using Archimedes Principle. ASTM International, nd

https://doi org/101520/B0962-17. 2017.

19. Wheat E, Vlasea M, Hinebaugh J, Metcalfe C. Sinter structure analysis of titanium structures fabricated via binder jetting additive manufacturing. Materials & Design. 2018;156:167-83.

20. Wallin RF, Upman P. A Practical Guide to ISO 10993: Part 1–Introduction to the Standards. Medical Device and Diagnostic Industry Magazine. 1998;20:96-9.

21. Su M, Wang H, Zhou Q, Chen C, Liu K, Hao X. Relationship Between Porosity and Spacer Content of Open Cell Metal Foams. Transactions of the Indian Institute of Metals. 2020;73(3):667-73.

22. Yang D, Cui Y, Qiu G, Lu T, editors. Investigation of Effect of the Urea Content on the Pore Morphology, Porosity, and Mechanical Behavior of Porous Ti. TMS 2022 151st Annual Meeting & Exhibition Supplemental Proceedings; 2022 2022//; Cham: Springer International Publishing.

23. Akbarinia S, Sadrnezhaad SK, Hosseini SA. Porous shape memory dental implant by reactive sintering of TiH2-Ni-Urea mixture. Mater Sci Eng C Mater Biol Appl. 2020;107:110213.

24. Dezfuli SN, Sadrnezhaad SK, Shokrgozar MA, Bonakdar S. Fabrication of biocompatible titanium scaffolds using space holder technique. J Mater Sci Mater Med. 2012;23(10):2483-8.

25. Wang X-h, Li J-s, Hu R, Kou H-c. Mechanical properties and pore structure deformation behaviour of biomedical porous titanium. Transactions of Nonferrous Metals Society of China. 2015;25(5):1543-50.

26. Yoshida K, Mishina H, Sasaki S, Morita M, Mabuchi K. Mechanical Properties of Titanium Cermets for Joint Prostheses. Materials Transactions. 2006;47(2):418-25.

27. Minagar S, Berndt CC, Wang J, Ivanova E, Wen C. A review of the application of anodization for the fabrication of nanotubes on metal implant surfaces. Acta Biomater. 2012 Aug;8(8):2875-88. doi: 10.1016/j.actbio.2012.04.005. Epub 2012 Apr 25. PMID: 22542885.

28. Rasouli R, Barhoum A, Uludag H. A review of nanostructured surfaces and materials for dental implants: surface coating, patterning and functionalization for improved performance. Biomaterials Science. 2018;6(6):1312-38.

29. Alitabar M, Yoozbashizadeh H. Study on the morphology and photocatalytic activity of TiO2 nanotube arrays produced by anodizing in organic electrolyte with Ni, Na, and C as dopants. Journal of Solid State Electrochemistry. 2018;22(12):3883-93.

30. Ahmadi S, Riahi Z, Eslami A, Sadrnezhaad SK. Fabrication mechanism of nanostructured HA/TNTs biomedical coatings: an improvement in nanomechanical and in vitro biological responses. Journal of Materials Science: Materials in Medicine. 2016;27(10):150.

31. Van Bael S, Chai YC, Truscello S, Moesen M, Kerckhofs G, Van Oosterwyck H, et al. The effect of pore geometry on the in vitro biological behavior of human periosteum-derived cells seeded on selective laser-melted Ti6Al4V bone scaffolds. Acta Biomaterialia. 2012;8(7):2824-34.

32. Čapek J, Vojtěch D. Properties of porous magnesium prepared by powder metallurgy. Materials Science and Engineering: C. 2013;33(1):564-9.

33. Siddiqui DA, Jacob JJ, Fidai AB, Rodrigues DC. Biological characterization of surface-treated dental implant materials in contact with mammalian host and bacterial cells: titanium versus zirconia. RSC Advances. 2019;9(55):32097-109.

34. Gui N, Xu W, Myers DE, Shukla R, Tang HP, Qian M. The effect of ordered and partially ordered surface topography on bone cell responses: a review. Biomaterials Science. 2018;6(2):250-64.